Available online at www.sciencedirect.com
SCIENCE DIRECT®
Physica C 390 (2003) 160–166
PHYSICA C
www.elsevier.com/locate/physc

Normal state Hall effect in $Nd_{1-x}Ca_xBa_2Cu_3O_{7-\delta}$: competition between added charge and disorder

S.R. Ghorbani *, M. Andersson, Ö. Rapp

Solid State Physics, IMIT, Royal Institute of Technology, KTH Electrum 229, SE-164 40 Kista-Stockholm, Sweden

Received 4 October 2002; received in revised form 6 January 2003; accepted 13 January 2003

Abstract

The transport properties of sintered samples of $Nd_{1-x}Ca_xBa_2Cu_3O_{7-\delta}$ with $0 \leqslant x \leqslant 0.20$ have been studied in the normal state by Hall resistivity measurements. The Hall coefficient, $R_H(x,T)$ was well described in terms of two different models. In a phenomenological narrow band model, the conduction band width became narrower with increasing Ca concentration while the density of states band width decreased slightly. A competition between two effects (i) added charge, and (ii) disorder introduced into the CuO_2 planes by doping, could be the main reason for the observed small decrease of the band widths. In the Anderson model, the temperature dependent part of the Hall angle was independent of hole concentration and disorder while the temperature independent part increased linearly with increasing Ca content. The results in both models support that Ca introduces disorder in the CuO_2 planes.

PACS: 74.72.Jt; 74.25.Fy; 74.62.Dh
Keywords: Hall coefficient; $Nd_{1-x}Ca_xBa_2Cu_3O_{7-\delta}$; Electronic band widths

1. Introduction

Normal state charge transport such as the resistivity, ρ, and the Hall effect in high-temperature superconductors is expected to be important for understanding the mechanism of high-temperature superconductivity (HTS). The electronic structure, carrier density, and scattering mechanisms are probed by such measurements. Studies of the normal state properties have been accordingly conducted since the discovery of HTSC [1]. However, there is still no consensus on the explanation of the observed experimental results. These properties are often inconsistent with the Fermi-liquid (FL) theory [2], and exhibit complicated dependence on temperature [3], charge doping [4,5], and disorder [6].

Several models have been proposed to describe the Hall effect, e.g. a temperature-dependent charge carrier density [7], magnetic skew scattering [8,9], and Anderson's Luttinger-liquid model [6, 10]. A phenomenological narrow band model of the electronic band structure of high-T_c superconductors has also been introduced [11], which in addition to electronic transport properties also has been used to describe the magnetic susceptibility, and the metal insulator transition [11–14].

* Corresponding author. Tel.: +46-8-790-4187; fax: +46-8-752-7850.
E-mail address: ghorbani@ftf.kth.se (S.R. Ghorbani).

0921-4534/03/$ - see front matter
doi:10.1016/S0921-4534(03)00700-7

It is known that substitution of Ca on the rare earth, RE, atom sites affects the superconducting properties of the RE-123 systems in a specific way. Ca restores superconductivity if it was previously suppressed by substitutions of Al or Co at the chain copper site, Cu1 [15,16], La and Nd at the Ba sites [16–18], or by oxygen reduction [19]. From studies of transport properties, it was found that at constant x in $Y_{1-x}Ca_xBa_2Cu_3O_y$, decreasing y results in increasing thermoelectric power S [20] and Hall coefficient R_H [21]. At fixed y, S and R_H are reduced by increasing x [22].

In this paper we present measurements of the normal state Hall coefficient R_H in Ca-doped Nd-123 from the superconducting T_c to room temperature. The Hall coefficient data were found to be well described by the phenomenological narrow band model of Ref. [14] over the whole temperature range above 96 K and the results were compared with those in other 123 compounds. This model has been chosen in the present case since it offers the possibility to describe experimental data of both $\rho(T)$, $R_H(T)$ and $S(T)$ in the normal state as a function of temperature with a set of closely related parameters. It was found that the width of the conduction band and the density of states decreased with increasing Ca concentration. Increased Ca doping also decreased band filling of electrons and produced asymmetry of the conduction band. This model description suggests that disorder is introduced in the CuO_2 planes by Ca doping. When the results were analyzed in the Anderson model [10] it was found that the temperature independent part of the Hall angle increased linearly by increasing Ca doping which also suggests that disorder is introduced by this doping.

2. Experimental

Samples with the composition $Nd_{1-x}Ca_xBa_2Cu_3O_{7-\delta}$ ($0 \leqslant x \leqslant 0.2$) were prepared by a standard solid state powder processing technique. High purity powders Nd_2O_3, $BaCO_3$, CuO, and $CaCO_3$ were first dried and then mixed in required proportions and ground. The samples were pressed into pellets and calcinated in air at 900, 920, and 920 °C with intermediate grindings. Finally, the samples were annealed in flowing oxygen at 460 °C for three days and the temperature was decreased to room temperature at a rate of 12 °C/h. X-ray diffraction (XRD) analysis was used to characterize the samples. The XRD results for Ca-doped Nd-123 showed that all samples had a single-phase orthorhombic 123 structure.

The electrical resistivity and Hall voltage were measured by standard four and five contact configurations, respectively using a field sweep technique with magnetic fields up to 8 T. Therefore, the Hall voltage and resistivity could be measured at the same time in one magnetic field sweep at each temperature. The temperature was regulated to within ±10 mK during each field sweep. Electrical leads were attached to the sample by silver paint and heat treated at 300 °C in flowing oxygen for half an hour, which gave contact resistances of order 1–2 Ω. The measurements were made on sintered bars of typical dimensions $0.5 \times 2.5 \times 6$ mm^3. The Hall voltage V_H as a function of the magnetic field B for $Nd_{1-x}Ca_xBa_2Cu_3O_{7-\delta}$ was linear for all sample for temperatures above T_c and magnetic fields up to 8 T. The Hall coefficient, R_H, was calculated from the slope of this relation.

3. Results and discussion

Fig. 1 shows R_H as a function of temperature and Ca concentration for $Nd_{1-x}Ca_xBa_2Cu_3O_{7-\delta}$. R_H is positive in the normal state for all samples and increases with decreasing temperature, has a maximum close 100 K for all samples and decreases strongly when approaching T_c. The results also show that R_H in $Nd_{1-x}Ca_xBa_2Cu_3O_{7-\delta}$ decreases with increasing x. The room temperature resistivity $\rho_{290\,K}$, which is shown in the inset of Fig. 1, also decreases with x. These results for R_H and $\rho_{290\,K}$ reflect that the hole concentration increases continuously with increasing Ca concentration. When the hole concentration further increases into the overdoped region, the temperature dependence of R_H appears to become less pronounced. The Hall coefficient in the normal state was analyzed within both a phenomenological narrow band model [14] and the Anderson model [10].

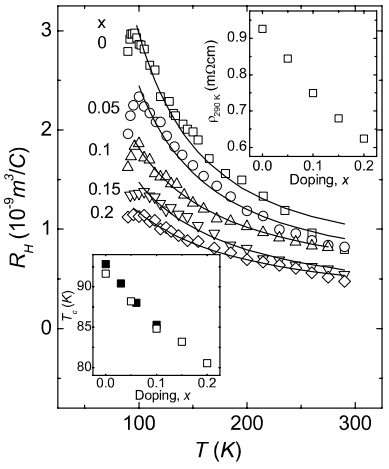

Fig. 1. The temperature dependence of the Hall coefficient R_H, for $Nd_{1-x}Ca_xBa_2Cu_3O_{7-\delta}$. The solid curves are fits to Eqs. (1) and (2). Inset (top right): The room temperature resistivity $\rho_{290\,K}$ as a function of Ca doping concentration, x. Inset (lower left): T_c versus x for present samples (□) and for data from Ref. [27] (■).

3.1. Phenomenological narrow band model

In the phenomenological narrow band model [14], it was found that all the features of the resistivity $\rho(T)$, the thermoelectric power $S(T)$, and the Hall coefficient $R_H(T)$ for the Y-123 system in the normal state should be explained and described quantitatively on the basis of a band model that assumed the existence of a narrow peak in the electronic density of state $D(E)$ close to the Fermi level. This model contains three main parameters for $\rho(T)$ and $S(T)$ and an additional one for $R_H(T)$: (i) the band filling by electrons, $F = n/N$, where n is the electron density and N is the total number of states in the band, (ii) the total effective band width w_D in $D(E)$, (iii) the conductivity effective band width w_σ in the longitudinal conductivity $\sigma(E)$, and (iv) for R_H the transverse effective band width $w_{\sigma H}$ in the transverse conductivity $\sigma_H(E)$. Using rectangular approximations for $D(E)$, $\sigma(E)$, and $\sigma_H(E)$, the result for R_H was

$$R_H = \frac{\langle\sigma_H\rangle}{\langle\sigma\rangle^2}\frac{(z-1)(v-1)^2(1+zu)^2(z+u)^2}{z(1+z)(z+v)(1+zv)(u^2-1)^2}, \qquad (1)$$

where $z = \exp(\mu^*)$, $v = \exp(\frac{w_{\sigma H}}{2k_BT})$, $u = \exp(\frac{w_\sigma}{2k_BT})$, and

$$\mu^* = \frac{\mu}{k_BT} = \ln\frac{\sinh\left(\frac{Fw_D}{2k_BT}\right)}{\sinh\left(\frac{(1-F)w_D}{2k_BT}\right)}, \qquad (2)$$

μ is the electron chemical potential and k_B the Boltzmann constant. $\langle\sigma\rangle$ and $\langle\sigma_H\rangle$ are the averages of the longitudinal conductivity and the transverse (Hall electrical) conductivity in the intervals w_σ and w_{σ_H}, respectively.

On the basis of a symmetric model it was found to be difficult to achieve good quantitative agreement between experimental results and model calculation of $S(T)$ for $Y_{1-x}Ca_xBa_2Cu_3O_y$ [23] and co-doped compounds of Ca and La(Co) in Y-123 [16,24] and $Bi_2Sr_2Ca_{2-x}Y_xCu_2O_y$ [25]. To analyse $S(T)$ data of high-T_c superconductors with Ca, the phenomenological narrow band model has been used with the additional assumption that the conduction band is asymmetric [16,23–25]. This would be caused by an additional peak in the density of states, $D(E)$ by Ca doping. At $x = 0$ the center of the rectangular approximations of $\sigma(E)$ and $D(E)$ coincide. With Ca doping such rectangular approximations to these two bands are shifted a distance bw_D. Fig. 2 illustrates how such a shift may arise from additional states in $\sigma(E,x)$. With this method, the expressions for $S(T)$ (Appendix A) and $R_H(T)$, Eqs. (1) and (2), are still valid if μ is replaced by $\mu - |b(x)|w_D$.

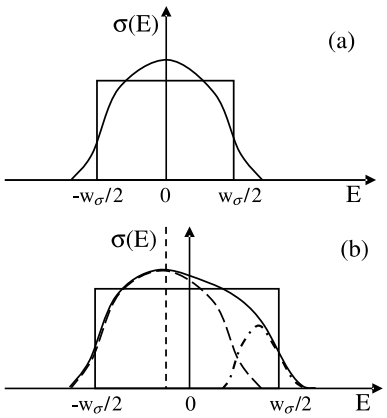

Fig. 2. Schematic electrical conductivity $\sigma(E)$ for (a) $x = 0$ and (b) $x > 0$ in $Nd_{1-x}Ca_xBa_2Cu_3O_{7-\delta}$. The dash-dot curve shows the contribution of the introduced additional states by Ca doping. The rectangle illustrates the model approximation of Ref. [14].

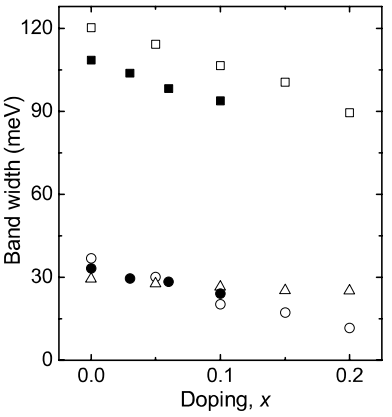

Fig. 3. Band width parameters as a function of Ca concentration, x, in $Nd_{1-x}Ca_xBa_2Cu_3O_{7-\delta}$; w_D (squares), w_σ (circles), and $w_{\sigma H}$ (triangles). Open symbols: present data. The solid symbols were calculated from thermoelectric power results in Ref. [27].

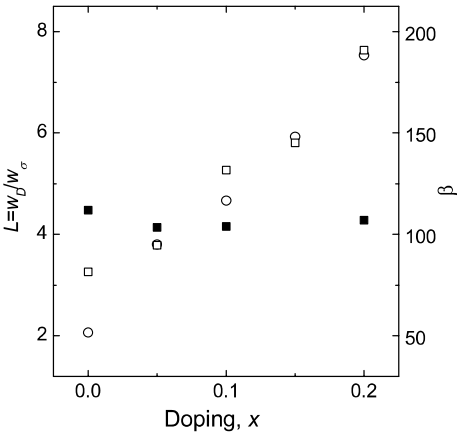

Fig. 4. Doping dependence of $L = w_D/w_\sigma$ (left hand scale) for $Nd_{1-x}Ca_xBa_2Cu_3O_{7-\delta}$ (□) and $YBa_{2-x}La_xCu_3O_y$ (■) from the phenomenological narrow band model. Hall angle parameter β versus x (right hand scale) for $Nd_{1-x}Ca_xBa_2Cu_3O_{7-\delta}$ (○) from the Anderson model. Data for $YBa_{2-x}La_xCu_3O_{7-\delta}$ have been obtained from Ref. [26].

The band widths in this model depend on the hole concentration [14,16,23–26]. By decreasing the hole concentration by oxygen reduction [14] or substitution of La on the Ba sites in Y-123 [26], the band width parameters increase and with increasing hole concentration they change in the opposite way [16]. We have fitted our $R_H(T)$ data to Eq. (1) as shown by the solid curves in Fig. 1 and estimated the band parameters. The band widths are shown in Fig. 3 (open symbols). All band widths (w_D, w_σ, and $w_{\sigma H}$) become somewhat narrower with increasing x. This is in agreement with the increasing hole concentration.

We also calculated the band widths from the thermoelectric power, from the relation $S(T, w_D, w_\sigma, F)$ (Appendix A), and data for $Nd_{1-x}Ca_xBa_2Cu_3O_y$ with $0 \leqslant x \leqslant 0.10$ from Ref. [27]. As can be seen in Fig. 3, the trend in w_D was stable, while the actual values for w_D obtained from $S(T)$ are somewhat smaller than for R_H. This is likely due to slightly different oxygen content as can be seen from the small differences in T_c for these series (see inset Fig. 1). The relation between T_c and w_D will be discussed below.

The tendency for Anderson localization at the band edges can be conveniently described by the parameter $L = w_D/w_\sigma$ [14]. The results for L are shown in Fig. 4. For $Nd_{1-x}Ca_xBa_2Cu_3O_{7-\delta}$, L increases linearly with x. This suggests an increasing tendency for localization and increasing electronic disorder for increased doping concentration. Such disorder would arise from the random occupation by Ca of some Nd sites in between the CuO_2 planes. Results for $YBa_{2-x}La_xCu_3O_y$ samples over a range of similar change of doping concentration [26] are also shown for comparison. In contrast to $Nd_{1-x}Ca_xBa_2Cu_3O_{7-\delta}$ there is no tendency for localization in $YBa_{2-x}La_xCu_3O_y$ where L is approximately constant.

The effect of Ca doping on the conduction band asymmetry b has been revealed by studies of $S(T)$ in co-doped $Y_{1-x}Ca_xBa_{2-x}La_xCu_3O_y$ [24] compounds with constant oxygen content. The electron density, n, was constant since added holes by Ca were compensated by La-doping, but $F = n/N$ decreased linearly with increasing x. Therefore, the total number of states in the conduction band, N, increased with x. In this case b increased linearly with increasing charge neutral doping level, x, suggesting that Ca doping changed the conduction band structure by inducing additional states [24].

Fig. 5 shows the conduction band asymmetry b and the band filling F as a function of x in $Nd_{1-x}Ca_xBa_2Cu_3O_{7-\delta}$. $|b|$ increased linearly with increasing Ca concentration. This is in agreement with

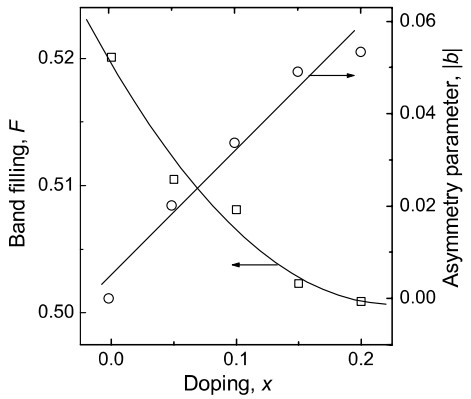

Fig. 5. Band filling by electrons F (left hand scale) and magnitude of band asymmetry b (right hand scale) versus Ca doping concentration, x, for $Nd_{1-x}Ca_xBa_2Cu_3O_{7-\delta}$. The curves are guides to the eye.

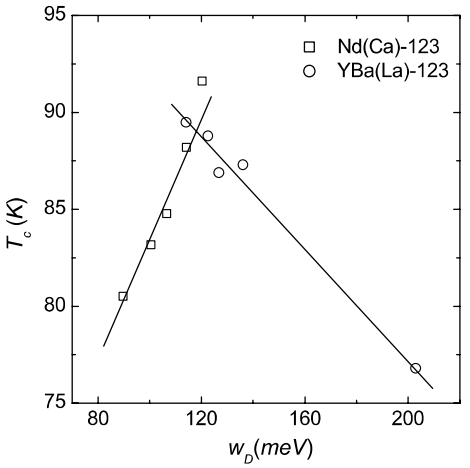

Fig. 6. The superconducting T_c versus the effective band width, w_D, for the present $Nd_{1-x}Ca_xBaCu_3O_{7-\delta}$ samples and $YBa_{2-x}La_xCu_3O_{7-\delta}$ [26].

results for b obtained from $S(T)$ in $Y_{1-x}Ca_xBa_2Cu_3O_y$ samples for increasing Ca concentration [23].

As can be seen in Fig. 5, F decreases with increasing Ca concentration. The increase in x thus leads to an increased hole density, consistent with the expectations from valence considerations. This result is expected from the results for R_H and $\rho_{290\ K}$ mentioned above. The number of states, N, also increases with increasing Ca concentration. Therefore, F is found to be nonlinear.

From studies of the thermoelectric power in doped Y-123 with different dopings, a correlation was found between the critical temperature T_c and the effective band width w_D, where T_c decreases with increasing w_D in the underdoped region [28]. Fig. 6 shows T_c as a function of w_D for the present $Nd_{1-x}Ca_xBa_2Cu_3O_{7-\delta}$ samples and for $YBa_{2-x}La_xCu_3O_{7-\delta}$ from Ref. [26] over a range of similar variation of T_c. T_c appears to have a maximum at $w_D \approx 120$ meV. With decreasing hole concentration in the underdoped region T_c decreased and w_D increased, while in the overdoped region both T_c and w_D decreased with increasing doping concentration. As can be seen in Fig. 6, the change in the band width at comparable depression of T_c is about 50% smaller for $Nd_{1-x}Ca_xBa_2Cu_3O_{7-\delta}$ ($dT_c/dw_D \approx 0.303$ K/meV) than for $YBa_{2-x}La_xCu_3O_{7-\delta}$ ($|dT_c/dw_D| \approx 0.145$ K/meV). The weak variation in w_D as a function of Ca doping concentration may result from a competition between two contributions. The first one is a weak increase of disorder in the CuO_2 planes as reflected in the parameter $L = w_D/w_\sigma$ (Fig. 4). This effect is absent in $YBa_{2-x}La_xCu_3O_{7-\delta}$. Weak disorder is expected to give a weak increase of w_D in $Nd_{1-x}Ca_xBa_2Cu_3O_{7-\delta}$. The second contribution is the increasing hole concentration which leads to a decrease in w_D. This contribution is the stronger one resulting in a weak decrease of w_D with Ca doping.

3.2. Anderson model

In the Anderson model [10], the conductivity in the longitudinal and transverse directions are governed by two different mechanisms and two different relaxation times due to spin-charge separation in the CuO_2 planes. The longitudinal (transport) relaxation time follows a linear T^{-1} dependence ($\tau_{tr} \propto T^{-1}$) and the transverse (Hall) relaxation time, follows a $\sim T^{-2}$ dependence ($\tau_H \propto T^{-2}$). τ_{tr} gives the well-known linear-T resistivity, ρ, while τ_H gives the temperature dependence of the Hall angle, $\cot\theta_H \propto T^2$. Allowing also for a temperature independent impurity contribution β one can write [10]:

$$\cot\theta_H = \rho/R_H B = \alpha T^2 + \beta, \tag{3}$$

α and β are constants.

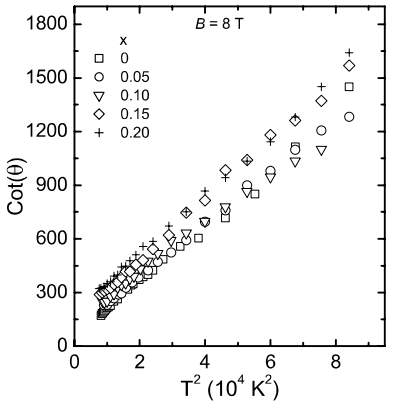

Fig. 7. T^2 dependence of $\cot\theta_H = \rho/R_H B$ in $B = 8$ T for $Nd_{1-x}Ca_xBa_2Cu_3O_{7-\delta}$ as a function of Ca concentration x.

Fig. 7 shows $\cot\theta_H$ vs. T^2 in a magnetic field, $B = 8$ T. The data were calculated from the results for $\rho(T)$ and $R_H(T)$. Irrespective of the complicated temperature dependencies of ρ [27] (for $x \leqslant 0.1$) and R_H (Fig. 1), a quadratic-like temperature dependence of $\cot\theta_H$ is obtained for all x values. A slight deviation from a T^2 dependence was observed at $T > 260$ K. α and β were determined from Fig. 7. The doping dependence of β for $Nd_{1-x}Ca_xBa_2Cu_3O_{7-\delta}$ is shown in Fig. 4. With increasing Ca concentration β increases linearly, whereas α was found to be constant within $\pm 7\%$ (not shown).

The doping dependence of α and β has been studied in $Y_{1-x}Ca_xBa_2Cu_3O_{7-\delta}$ thin films with $x = 0$–0.5 and $\delta = 0.08$–1 [29]. It was found that β increased monotonically with x, while α was independent of doping level and also independent of δ in the region of large oxygen reduction. From studies of nonmagnetic Zn doping on the magnetic Cu sites in single-crystal Y-123, Chien et al. [6] found that β increased linearly with increasing Zn concentration, whereas α was constant. Our results (Fig. 4) show that β increases linearly, which can be ascribed the creation of disorder in the CuO_2 plane by Ca doping in agreement with previous work [6,13,29]. The roughly constant α suggests that the temperature dependent part in Eq. (3) does not depend on the hole doping, disorder, or substitution of impurities (magnetic or nonmagnetic).

The two different models used to analyse $R_H(x,T)$ are based on different assumptions and therefore difficult to compare quantitatively. However, as mentioned both β in the Anderson model and the parameter L in the phenomenological narrow band model depend on disorder. The Ca concentration dependence of β and L are compared in Fig. 4. Both β and L increase linearly by a similar factor for doping concentrations up to $x = 0.2$. Therefore, these results support that Ca introduces disorder in the CuO_2 plane. The disorder gives a contribution in the direction of an increasing band width w_D, which weakens the decrease of w_D due to added charge.

4. Brief conclusion

The transport properties of sintered samples of $Nd_{1-x}Ca_xBa_2Cu_3O_{7-\delta}$ have been studied in the normal state. Both resistivity and Hall coefficient decreased with increasing Ca concentration. A phenomenological narrow band model could well describe the results for the Hall coefficient. On the basis of this model, as Ca doping concentration increased, the conduction band became narrower and the degree of band filling with electrons decreased. The degree of asymmetry of the band increased by induced additional states in the band. The results could also be analyzed in terms of the Anderson model, where the temperature dependence part of the Hall angle is roughly proportional to T^2 and independent of hole concentration and disorder. The results of both models indicated that Ca introduced disorder, which could be the main reason for the observed small decrease of the band widths in Ca doped 123 systems.

Acknowledgements

We would like to thank Ingrid Bryntse and M. Valldor, Stockholm University, for help with sample preparation and X-ray analyses. Financial support by the Swedish Agencies Vetenskapsrådet and the SSF Oxide program and from the Iranian Ministry of Science, Research, and Technology are gratefully acknowledged.

Appendix A

In the phenomenological narrow band model of Ref. [14], the thermoelectric power is expressed in term of the three parameters w_σ, w_D and F as

$$S = -\frac{k_B}{e}\left\{\frac{w_\sigma^*}{\sinh w_\sigma^*}\left[e^{-\mu^*} + \cosh w_\sigma^* - \frac{1}{w_\sigma^*}(\cosh\mu^* + \cosh w_\sigma^*)\ln\frac{e^{\mu^*} + e^{w_\sigma^*}}{e^{\mu^*} + e^{-w_\sigma^*}}\right] - \mu^*\right\},$$

$$\mu^* = \frac{\mu}{k_B T} = \ln\frac{\sinh(Fw_D^*)}{\sinh(1-F)w_D^*},$$

$$w_D^* = \frac{w_D}{2k_B T}, \quad \text{and} \quad w_\sigma^* = \frac{w_\sigma}{2k_B T}.$$

References

[1] N.P. Ong, Z.Z. Wang, J. Clayhold, J.M. Tarascon, L.H. Greene, W.R. McKinnon, Phys. Rev. B 35 (1987) 8807.
[2] P.W. Anderson, Science 235 (1987) 1196, 256 (1992) 1526.
[3] T.R. Chien, D.A. Brawner, Z.Z. Wang, N.P. Ong, Phys. Rev. B 43 (1991) 6242.
[4] T. Manako, Y. Kubo, Y. Shimakawa, Phys. Rev. B 46 (1992) 11019.
[5] T. Ito, K. Takenaka, S. Uchida, Phys. Rev. Lett. 70 (1993) 3995.
[6] T.R. Chien, Z.Z. Wang, N.P. Ong, Phys. Rev. Lett. 67 (1991) 2088.
[7] Y. Kubo, T. Kondo, Y. Shimakawa, T. Manako, H. Igarashi, Phys. Rev. B 45 (1992) 5553.
[8] A.T. Fiory, G.S. Grader, Phys. Rev. B 38 (1988) 9198.
[9] B. Wuyts, V.V. Moshchalkov, Y. Bruynseraede, Phys. Rev. B 53 (1996) 9418.
[10] P.W. Anderson, Phys. Rev. Lett. 67 (1991) 2092.
[11] V.V. Moshchalkov, Physica C 156 (1988) 473.
[12] V.V. Moshchalkov, Physica B 163 (1990) 59.
[13] C. Quitmann, D. Andrich, C. Jarchow, M. Fleuster, B. Beschoten, G. Güntherodt, V.V. Moshchalkov, G. Mante, R. Manzke, Phys. Rev. B 46 (1992) 11813.
[14] V.E. Gasumyants, V.I. Kaidanov, E.V. Valadimirskaya, Physica C 248 (1995) 255.
[15] R. Suryanarayanan, S. Leelaprute, L. Ouhammou, A. Das, J. Supercond. 7 (1994) 77.
[16] E.V. Valadimirskaya, V.E. Gasumyants, I.B. Patrina, Phys. Solid State 37 (1994) 1088.
[17] A.G. Joshi, D.G. Kuberkar, R.G. Kulkarni, Physica C 320 (1999) 87.
[18] K.M. Pansuria, D.G. Kuberkar, G.J. Baldha, R.G. Kulkarni, Supercond. Sci. Technol. 12 (1999) 579.
[19] V.P.S. Awana, S.K. Malik, W.B. Yalon, Physica C 262 (1996) 272.
[20] B. Fisher, J. Genossar, C.G. Kuper, L. Patlagan, G.M. Reisber, A. Knizhnik, Phys. Rev. B 47 (1993) 6054.
[21] I.R. Fisher, P.S.I.P.N. de Silva, J.W. Loram, J.L. Tallon, A. Carrington, J.R. Cooper, Physica C 235–240 (1994) 1497.
[22] T. Honma, K. Yamaya, Physica C 185–189 (1991) 1245.
[23] V.E. Gasumyants, V.V. Valadimirskaya, M.V. Elizarova, N.V. Ageev, Phys. Solid State 40 (1998) 1943.
[24] V.E. Gasumyants, M.V. Elizarova, I.B. Patarina, Supercond. Sci. Technol. 13 (2000) 1600.
[25] N.V. Ageev, V.E. Gasumyants, V.I. Kaidanov, Phys. Solid State 37 (1995) 1171.
[26] V.E. Gasumyants, E.V. Valadimirskaya, I.B. Patarina, Phys. Solid State 40 (1998) 14.
[27] S.R. Ghorbani, P. Lundqvist, M. Andersson, M. Valldor, Ö. Rapp, Physica C 339 (2000) 245.
[28] M.V. Elizarova, V.E. Gasumyants, Phys. Solid State 41 (1999) 1248.
[29] H. Yakabe, I. Terasaki, M. Kosuge, Y. Shiohara, N. Koshizuka, Phys. Rev. B 54 (1996) 14986.